

# Flow rate of granular media: Breakdown of the Beverloo's scaling

Marcos A. Madrid<sup>1</sup>, J. R. Darias<sup>2</sup>, Luis A. Pugnaloni<sup>1</sup>

<sup>1</sup>*Departamento de Ingeniería Mecánica, Facultad Regional La Plata, Universidad Tecnológica Nacional, CONICET, Av. 60 Esq. 124, 1900 La Plata, Argentina.*

<sup>2</sup>*Laboratorio de Óptica y Fluidos, Universidad Simón Bolívar, Apartado Postal 89000, Caracas 1080-A, Venezuela.*

The Beverloo's scaling for the gravity flow of granular materials through orifices has two distinct universal features. On the one hand, much highlighted in the literature, the flow rate is independent of the height of the granular column. On the other hand, less celebrated yet more striking, the flow rate is fairly insensitive to the material properties of the grains (density, Young's modulus, friction coefficient, etc.). We show that both universal features are lost if work is done on the system at a high rate. In contrast with viscous fluids, the flow rate increases during discharge if a constant pressure is applied to the free surface of a granular column. Moreover, the flow rate becomes sensitive to the material properties. Nevertheless, a new universal feature emerges: the dissipated power scaled by the mean pressure and the flow rate follows a master curve for all conditions of forcing and material properties studied. We show that this feature can be explained if the granular flow in the silo is assumed to be a quasistatic shear flow.

PACS numbers: 45.70.-n, 45.70.Mg

The flow of granular matter (bulk solids such as sand, seeds, pellets, etc.) presents rather peculiar features when compared with viscous fluid flows. Prompted by the numerous industrial applications and by academic curiosity, an entire area of research has been developed around granular matter. Despite numerous advances, we are still far from producing a synthesis to provide a theoretical framework that can be applied to all phenomena observed in granular matter. Instead, we are still gaining knowledge from focusing on a particular experimental observation and pushing to the limit our yet incomplete models. One archetypal phenomenon in this sense is the discharge of granular materials through an orifice at the bottom of a silo. This has been considered in a number of studies since the 19th century (see for example [1–3] and references therein). The most salient feature, usually highlighted in the literature, is the fact that the flow rate does not depend on the height  $h$  of the column of grains in the container, in clear contrast with the behavior of viscous fluids. A much more striking peculiarity, yet little mentioned, is that the flow rate is not affected by the material the grains are made of [2]. This latter “universality” is still poorly understood.

If the discharge orifice is circular and large enough to avoid clogging [4], the mass flow rate  $W$  is described by the so called Beverloo's rule [2, 5]

$$W = C\rho_b\sqrt{g}(D - kd)^{5/2}, \quad (1)$$

where  $D$  is the diameter of the opening,  $\rho_b$  the bulk density of the granular sample,  $g$  the acceleration of gravity and  $d$  the diameter of the grains. Here,  $k$  and  $C$  are two fitting dimensionless constants. Interestingly, while  $k$  may vary up to a factor of 2, depending on the shape of the grains used,  $C \approx 0.58$  for virtually any material tested. Initially, Beverloo et al. [2], and more recently

Kondic [6] and Mankoc et al. [7] have stressed this point. Even though this material independence is not a fundamental law of nature for the flow of grains, it is in fact a remarkable emerging feature still little investigated. Notice that Eq. (1) does include  $\rho_b$ , which depends on the material density of the grains. However, this is only to calculate the mass flow rate  $W$ . The particle flow rate  $Q = W/m$ , with  $m$  the mass of one grain, does not depend on the density of the material.

A simple explanation for the  $5/2$  power in the Beverloo's rule is based on an heuristic assumption so called *free fall arch* [3]. It states that most grains lose contact with the rest of the granular packing when they reach a position that is about one orifice radius,  $D/2$ , above the outlet and that particles at this point fall freely from an initial zero vertical velocity. Then, the free fall of these grains over a distance  $D/2$  leads to a flow rate proportional to  $\sqrt{g}D^{5/2}$ , irrespective of their material properties.

In this letter, we show that adding a piston on top of the granular column the universal feature described above breaks down. We observed that, when forced, the flow rate increases during the discharge (in contrast with viscous fluids) and the change in  $Q$  depends on the material properties of the grains. We will show that, for different materials and forcing conditions, the dissipated power scaled by the mean internal pressure in the silo and by the flow rate, falls onto a single master curve as a function of the number of grains remaining in the silo. This scaling is consistent with the assumptions made for a quasistatic shear flow in the so called  $\mu(I)$ -rheology, based on the introduction of the inertial number  $I$  [8]. The analysis of these extreme conditions of discharge allows us to put forward some ideas that help in understanding the limits of the *free fall arch* model [3] and the

universal features of the unforced discharge.

**Experiments**— The experimental setup is shown in Fig. 1(a). The silo is a cylindrical glass tube ( $300 \pm 1$ ) mm tall and  $(40.0 \pm 0.5)$  mm in internal diameter, which is attached to a metal stand that holds it fixed. The bottom of the tube is bonded to an aluminum base that has a central orifice ( $15.0 \pm 0.5$ ) mm in diameter. The silo is filled to a height ( $190 \pm 1$ ) mm by pouring uniformly glass beads with diameter  $(1.00 \pm 0.05)$  mm and bulk density  $(1600 \pm 20)$  kg/m<sup>3</sup>. We introduce a solid cylinder (piston) of Plexiglas ( $37 \pm 1$ ) mm tall,  $(39.50 \pm 0.05)$  mm in diameter and mass  $(130 \pm 1)$  g, which serves as a support for an extra overweight that can be placed on top. The downward motion of the piston was recorded using a digital camera (Pixelink PL-B741F) at 25 fps. The images were analyzed using a commercial software to obtain the height of the column of grains as a function of time. This allow us to calculate  $W(t)$  under the approximation that the packing fraction is roughly constant during the discharge. The internal friction coefficient of the glass beads is  $\mu = 0.40 \pm 0.03$ .

**Simulations**— Most of the analysis is done on Discrete Element Method (DEM) simulations. We use the implementation of YADE [13] with a particle–particle interaction comprising a linear spring–dashpot model for the normal,  $F_n = k_n \xi - \gamma_n \dot{\xi}$ , and tangential,  $F_t = \min(\mu F_n, k_t \zeta - \gamma_t v_t)$ , contact forces. Here,  $\xi$  is the particle–particle overlap,  $\zeta$  the total shear displacement of the contact and  $v_t$  the relative tangential velocity. Unless otherwise specified,  $k_n = 1000$  Nm<sup>-1</sup>,  $k_t = 2k_n/7$ ,  $\gamma_n = 0.03$  Nsm<sup>-1</sup>,  $\gamma_t = 0.02$  Nsm<sup>-1</sup> and  $\mu = 0.55$ . The same interaction applies for the particle–walls contacts.  $N = 5 \times 10^4$  spherical grains (diameter  $d = 1$  mm) are poured in a silo. The sphere material density,  $\rho$ , was set to different values (500, 1000 and 2000 kg/m<sup>3</sup>). The silo has a diameter  $D_s = 2R_s = 30d$  with an orifice of diameter  $D = 15d$  at the center of the base. The orifice is initially blocked by a plug. After the grains come to rest in the silo (we wait until the kinetic energy per particle falls below  $10^{-6}$  J), we remove the plug and count the number of grains that pass through the aperture per unit time. The acceleration of gravity  $g = 9.81$  ms<sup>-2</sup> acts in the negative vertical direction. For the forced flow simulations, we introduce a cylindrical piston (78.54 g) made of small spheres ( $0.33d$  in diameter) whose relative positions are fixed during the simulation.

**Results**— Figure 1(b) shows the experimental mass flow rate for glass beads for forced discharges using different overweights. As we can see, for light overweights (with exception of the lighter overweight tested),  $W$  is constant during the initial part of the discharge and then grows in the final stages of the discharge. As the overweight becomes heavier, the acceleration of the mass flow rate is more significant and starts at an earlier stage. In contrast with viscous fluids, which decrease in flow rate as the column empties (even with an external constant

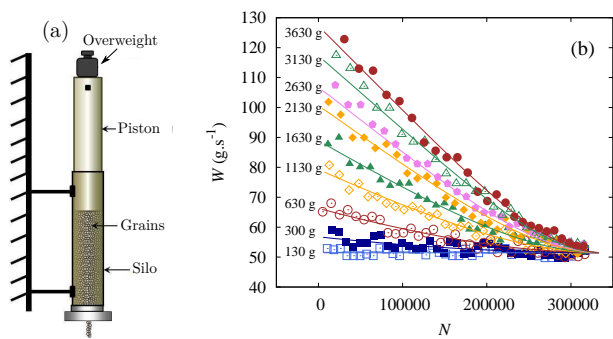


FIG. 1. (Color online) (a) Sketch of the experimental setup. (b) Mass flow rate  $W$  as a function of the number of grains  $N$  left in the silo measured in the experiments during the forced discharge of glass beads for different overweights (see labels in the figure). The full lines are only to guide the eye. Each curve corresponds to the average over six realizations of the experiment.

forcing), granular samples forced with a constant applied force increase their mass flow rate. This striking behavior is consistent with enhanced flows observed in similar experiments carried out by Peng et al. [14]. Wilson et al. showed a similar growth in  $Q$  for a submerged silo (interestingly, without the need of extra overweight) [15]; however, this was latter proven to be due to an hydrodynamic effect [16]. One may speculate that the overweight induces a higher pressure at the bottom of the silo (as shown by other authors [17]) and this is responsible for the increased flow rate. We will discuss this below. Importantly, the increasing mass flow rate suggests that forced discharges cannot longer be explained by a simple *free fall arch* assumption and that properties related to the specific material the grains are made of may become relevant in the problem. Since we find difficult varying material properties in the experiments in a controlled way, we turn in the rest of the discussion into results obtained via the DEM simulations.

Figure 2(a) shows the particle flow rate during the discharge of grains with different material properties, without external forcing, obtained via DEM simulations. We have removed from the analysis the transients at the beginning and end of the discharge by ignoring the initial and final 5000 grains. As we can see,  $Q$  is constant throughout the discharge and the actual values do not depend on the material properties. These observations are consistent with results from many other authors that studied free discharges. Note, however, that the sample with  $\mu = 0.31$  do display an slightly higher  $Q$  which is still independent of  $h$  as seen recently by others in the case of low friction [6]. The pressure at the bottom of the silo during the discharges is shown in Fig. 2(c). It is clear that the bottom pressure falls monotonically throughout the discharge while the flow rate remains constant. This has been highlighted in previous studies [10, 11].

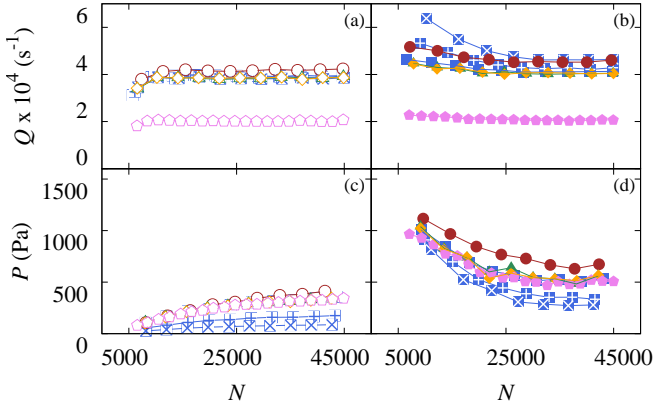


FIG. 2. (Color online) Particle flow rate  $Q$  (panels (a) and (b)) and bottom pressure  $P$  (panels (c) and (d)) as a function of the number of particles  $N$  in the simulated silo discharge. Open symbols correspond to unforced discharges (panels (a) and (c)) and solid symbols to forced discharges with an overweight of 78.54 g (panels (b) and (d)). Each curve corresponds to a different material:  $\rho = 2000 \text{ kg/m}^3$ ,  $\mu = 0.31$  (red circles);  $\mu = 0.55$  (blue squares);  $\mu = 0.85$  (green triangles);  $\mu = 1.0$  (orange diamonds);  $\rho = 1000 \text{ kg/m}^3$ ,  $\mu = 0.55$  (blue squares with pluses);  $\rho = 500 \text{ kg/m}^3$ ,  $\mu = 0.55$  (blue squares with crosses). Most discharges are for an orifice diameter  $D = 15.0 \text{ mm}$ . The pink pentagons correspond to a smaller orifice (12.0 mm) with  $\rho = 2000 \text{ kg/m}^3$  and  $\mu = 0.55$ .

In Fig. 2(b), we show results for the flow rate during the discharge of a silo with an overweight (roughly 1.5 times that of the material inside the container). The results are consistent with the experiments (see open circles in Fig. 1), showing an increase of  $Q$  towards the end of the discharge. Fig. 2(d) shows that the bottom pressure increases during the discharge since the portion of granular column screening the overweight decreases. Results for different overweightings can be found in the Supplemental Material [21].

An interesting result is that in the forced discharges, apart from the accelerating  $Q$ , the actual acceleration becomes dependent on the material properties of the grains. For example, Fig. 2(b) shows that denser materials present a lower  $Q$  during the acceleration phase. This seems counterintuitive since the heavier grains induce in fact a higher bottom pressure (see Fig. 2(d)). We will put forward an explanation for this effect below. The friction coefficient also affects, although to a lesser extent, the values of  $Q$  achieved during the speedup. The larger the friction coefficient, the lower is the speedup of  $Q$  (compare filled orange diamonds and filled blue squares in Fig. 2(b)). We conclude that the universal character of the Beverloo's rule, in which the particle flow rate is insensitive to the material properties, breaks down in forced flows.

One may speculate that the increased pressure in the bottom of the silo due to the use of a piston is the ultimate responsible for the increase in  $Q$ . However, there

are a few observations that indicate that this is not the case. For the unforced discharges, materials with different density induce very different pressures on the base, yet the flow rate is insensitive to this [18]. For forced discharges, the bottom pressure increases during the discharge. However, even higher bottom pressures can be also achieved without an overweight (either by using a wider silo or by discharging materials with very high densities). In these free flow case,  $Q$  always coincides with the one obtained for any unforced discharge for the given  $D$ , which is lower than the enhanced  $Q$  seen in the forced discharges. Although pressure is a relevant parameter of the problem, it is clear that it does not control the flow rate on its own.

*Dissipated power*— The flow in a discharging silo could be connected with simpler geometries, such as a shear cell, where valuable scalings have been found. It has been shown that for a shear cell of thickness  $L$  the tangential stress  $\tau$  necessary to develop a flow at velocity  $v$  of a granular sample can be put in terms of the inertial number  $I$  as [19]

$$\tau = \mu(I)P, \quad (2)$$

where  $P$  is the confining pressure,  $\mu(I)$  is the effective friction coefficient,  $I = \frac{v}{L} \frac{d}{\sqrt{P/\rho}}$  is the inertial number that characterizes the flow (if the grains are stiff and  $L \gg d$ ) and  $\rho$  is the density of the material of the grains. We assume here that the flow in the silo can be roughly represented as a shear flow, where  $v$  is the velocity of the free surface,  $L$  is the silo radius and  $P$  is the mean stress in the column [20]. Then, we can write the power,  $W_D$ , dissipated by friction at any given time during the discharge as

$$\begin{aligned} W_D(t) &= \tau(t)A(t)v(t) = \mu(I)P(t)A(t)v(t) \\ &= \mu(I)P(t)A(t) \frac{Q(t)m}{\rho_b A_s}, \end{aligned} \quad (3)$$

where  $A(t)$  is the area of frictional contact between the grains and the silo,  $A_s$  is the cross section of the silo, and we have used the continuity relation  $W(t) = mQ(t) = \rho_b A_s v(t)$ .

In Eq. (3),  $A(t)$  includes the contact with the lateral walls, which decreases during the discharge, plus a fixed area due to the effect of the base of the silo. Hence, we can express  $A(t)$  as

$$A(t) = 2\pi R_s z(t) + \alpha \pi R_s^2, \quad (4)$$

where  $R_s$  is the silo radius,  $z(t)$  is the height of the granular column at time  $t$ , and  $\alpha$  is a constant to correct the frictional area of the base due to the cone generated by the stagnant zone. Further, we can put

$z(t)$  in terms of the number of grains in the silo as  $z(t) = mN(t)/(\rho_b \pi R_s^2)$ .

We can show that  $\mu(I)$  is insensitive to the granular material properties. Consider  $A_s \rightarrow \infty$ , then  $L \rightarrow \infty$  and  $I \rightarrow 0$ . Da Cruz *et al.* have shown that in the quasistatic limit (i.e.,  $I \rightarrow 0$ )  $\mu(I \rightarrow 0) \approx 0.26$  for all material properties if the grain-grain friction coefficient is above 0.4 [19]. In our simulations with a finite diameter silo the inertial number varies during the discharge in the range  $9.8 \times 10^{-3} < I < 1.6 \times 10^{-2}$ , which is indeed in the quasistatic limit ( $I < 10^{-2}$ ) [19]. Therefore, from Eqs. (3) and (4),

$$\frac{W_D}{PQ}(t) = 0.26 \frac{m}{\rho_b} \frac{A(t)}{A_s} = 0.26 \frac{m}{\rho_b} \left[ \frac{m}{\pi R_s^3} 2N(t) + \alpha \right], \quad (5)$$

which is a quantity that should not depend on the material properties, nor forcing conditions, nor orifice size  $D$ . Note that  $\rho_b/m$  is the number density, which does not depend on the density of the material of the grains.

Figure 3 shows  $W_D/(PQ)$  as a function of the number of grains in the silo for all the discharges, forced and unforced, for all the values of  $\rho$  and  $\mu$  considered. We have also included results for a discharge with a smaller orifice (see pink pentagons in Fig. 3). With exception of the low friction sample ( $\mu = 0.31$ , red filled circles), all curves fall into a single straight line (although with some scatter) that can be fitted reasonably well with Eq. (5), where the only free parameter is  $\alpha$  (see full line in Fig. 3). For  $\mu = 0.31$ , the observed deviation from Eq. (5) is expected since  $\mu(I \rightarrow 0)$  does depend on  $\mu$  for  $\mu < 0.4$ . Equation (5) indicates that the slope of the straight line is inverse to  $R_s^3$ . Results for different silo radii, confirming this prediction, can be found in the Supplemental Material [21]. The scaling shown by Fig. 3 demonstrates that the flow in a silo discharge could be modeled as a quasistatic flow, for unforced and forced conditions, without the need of heuristic postulates such as the *free fall arch*. A first modeling attempt in this direction, considering only free discharges, can be found in Ref. [22].

*Discussion*— From a “microscopic” perspective, we can understand the lack of dependency on the material properties for free discharges based on an *effective inelastic collapse* [23]. When the density is high, the number of collisions per unit time grows exponentially with the number of particles. As a consequence, even if individual collisions dissipate little energy, the kinetic energy of the entire system will be damped in a very short time. If the system is in a state of *effective inelastic collapse*, any work done on the grains inside the silo will be dissipated in a very short time (in particular the work done by the force of gravity). Therefore, with the exception of the grains that set free from the pack as they reach the region of the aperture, the system inside the silo moves, as a whole, at constant velocity. The flow rate consistent with such velocity is imposed solely by the size of

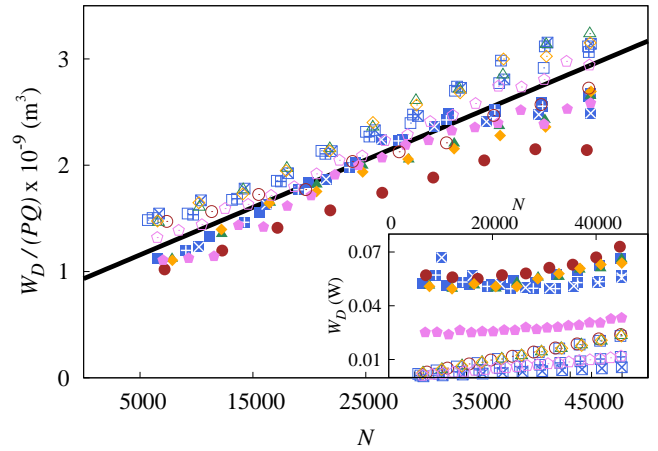


FIG. 3. (Color online)  $W_D/(PQ)$  during a discharge as function of the number  $N$  of particles in the silo for different material properties, orifice size and forcing conditions (symbols as in Fig. 2). The inset shows  $W_D$  as a function of  $N$ . The solid line corresponds to the best fit to Eq. (5) yielding  $\alpha = 3.76$ .

the orifice, without the influence of the local or global pressure.

The increase in  $Q$  for forced discharges can be attributed to the loss of *effective inelastic collapse*. Since the piston is doing work on the system at a high rate and the total number of contacts (collisions) decreases during the discharge, these fewer contacts are eventually unable to fully dissipate the energy input. As a result, the flow rate increases due to the not dissipated kinetic energy. We suggest that the same phenomenon occurs even in unforced discharges. However, the work done by the gravity force is low and decreases as the silo discharges, so the accelerated  $Q$  would be observed only when a very small number of particles remain in the silo. Indeed, this is consistent with previous preliminary observation [15, 16, 24] although no systematic study of the phenomenon has been carried out to our knowledge.

The previous picture is consistent with the results in Fig. 2 for forced flows. On the one hand, more dissipative materials (higher  $\mu$ ) display a slower acceleration in  $Q$  as should be expected. On the other hand, denser grains display a slower increase in  $Q$ , which is unexpected. Consider however that heavier grains induce a higher average pressure across the packing. This is consistent with stronger contact forces which lead to higher dissipation by friction at each contact for a given  $\mu$ , since the tangential force is proportional to the normal. As a consequence, denser grains are able to dissipate more of the injected power and the increase in  $Q$  is delayed until fewer particles remain in the column to dissipate the energy.

*Conclusions*— Despite the little attention received, the universal free flow rate of granular materials with respect to the different material properties is a remarkable phe-

nomenon. By injecting energy into the system at a high rate, we have shown that not only the independence of  $Q$  with the system height is broken, also the universality with respect to material properties is lost. In contrast with viscous fluids, the flow rate is accelerated during the discharge due to the reduction of dissipation as the number of grains decreases in the container.

We have shown that for both, forced and unforced discharges, the flow can be described as a shear flow consistent with the  $\mu(I)$ -rheology in the quasistatic limit; where the flow does not depend on the material properties of the grains if the grain-grains friction coefficient is above 0.4. This opens the opportunity for modeling silo discharges in a wide range of conditions without the need of heuristic approximations such as the *free fall arch* and the *empty annulus*, which have been recently challenged [25, 26].

We are grateful for valuable discussions with D. Maza, L. Kondic, I. Zuriguel, J.-C. Géminard, M. A. Aguirre, D. Durian and E. Clément. This work has been supported by ANPCyT (Argentina) through grant PICT-2012-2155, Universidad Tecnológica Nacional (Argentina) through grant PID-MA0FALP0002184, Centro Argentino Francés de Ciencias de la Ingeniería (CAFCI, Argentina-Francia) and FONACIT through grant 2015000072 (INVUNI2013-1563) Universidad Simón Bolívar (Venezuela).

- 
- [1] L. P. Kadanoff, *Rev. Mod. Phys.* **71**, 435 (1999); P. G. de Gennes, *Rev. Mod. Phys.* **71**, S374 (1999); H. M. Jaeger, S. R. Nagel and R. P. Behringer, *Rev. Mod. Phys.* **68**, 1259 (1996); J. Duran, *Sands, Powders and Grains*, Springer, New York, (2000); B.P. Tighe and M. Sperl, *Gran. Matt.* **9**, 141-144 (2007).
  - [2] W. A. Beverloo, H. A. Leninger and J. van de Valde, *Chem. Eng. Sci.* **15**, 260 (1961)
  - [3] R. M. Nedderman, *Statics and kinematics of granular material*, Cambridge University Press, New York (1992).
  - [4] I. Zuriguel, L. A. Pugnaloni, A. Garcimartín and D. Maza, *Phys. Rev. E* **68**, 030301(R) (2003).
  - [5] R. L. Brown and J. C. Richards, *Principles of Powder Mechanics*, Pergamon Press, Oxford, (1970).
  - [6] L. Kondic, *Granular Matter* **16**, 235-242 (2014).
  - [7] C. Mankoc, A. Janda, R. Arévalo, J. M. Pastor, I. Zuriguel, A. Garcimartín and D. Maza, *Gran. Matt.* **9**, 407-414 (2007).
  - [8] F. da Cruz, S. Emam, M. Prochnow, J. N. Roux, and F. Chevoir, *Phys. Rev. E* **72**, 021309 (2005).
  - [9] L. Staron, P.-Y. Lagre, and S. Popinet, *Phys. Fluids* **24**, 103301 (2012).
  - [10] M. A. Aguirre, J. G. Grande, A. Calvo, L. A. Pugnaloni, and J.-C. Géminard, *Phys. Rev. Lett.* **104**, 238002 (2010).
  - [11] M. A. Aguirre, J. G. Grande, A. Calvo, L. A. Pugnaloni, and J.-C. Géminard, *Phys. Rev. E* **83**, 061305 (2011).
  - [12] C. Perge, M. A. Aguirre, P. A. Gago, L. A. Pugnaloni, D. Le Tourneau, and J.-C. Géminard, *Phys. Rev. E* **85**, 021303 (2012).
  - [13] V. Smilauer, E. Catalano, B. Chareyre, S. Dorofeenko, J. Duriez, A. Gladky, J. Kozicki, C. Modenese, L. Scholtés, L. Sibille, J. Stránský, and K. Thoeni, Yade Documentation. The Yade Project. (<http://yade-dem.org/doc/>) (2010).
  - [14] Z. Peng, H. Zheng, and Y. Jiang, arXiv:0908.0258v3 (2009).
  - [15] T. J. Wilson, C. R. Pfeifer, N. Mesyngier, and D. J. Durian, *Papers in Physics*, **6**, 060009 (2014).
  - [16] J. Koivisto and D. J. Durian, arXiv:1602.05627v3 (2016).
  - [17] G. Ovarlez and E. Clément, *Eur. Phys. J. E* **16**, 421 (2005).
  - [18] This is in line with a remark by Staron et al. [9] that show that the pressure at the silo base can be changed by using silos of different diameters, however the flow rate remains the same.
  - [19] F. da Cruz, S. Emam, M. Prochnow, J. N. Roux, and F. Chevoir, *Phys. Rev. E* **72**, 021309 (2005).
  - [20] The pressure in a granular column varies significantly as a function of the vertical coordinate. Also the shear rate (estimated by measuring the difference in mean velocity of the grains at the central axis and the grains close to the walls and dividing by the silo radius) is different at different heights during a discharge. For a flat bottomed silo discharging with a mass flow regime, close to the free surface the shear rate is negligible. However, close to the base, the shear rate is maximum since the velocity at the walls is zero (due to the stagnant zone) and the velocity at the outlet is the highest. Taking the velocity at the free surface and averaging the pressure over the entire column is a rather crude approximation. However, the scaling found in this work is already good. Improvements can be made by taking a layer-wise approach.
  - [21] See Supplemental Material below.
  - [22] M. A. Madrid, J. R. Darias, L. A. Pugnaloni, arXiv: (2016).
  - [23] S. McNamara, W.R. Young, *Phys. Fluids A* **4** 496-504 (1992).
  - [24] J.-Ch. Géminard (private communication, 2010).
  - [25] A. Janda, I. Zuriguel and Diego Maza, *Phys. Rev. Lett.* **108**, 248001 (2012).
  - [26] S. M. Rubio-Largo, A. Janda, D. Maza, I. Zuriguel and R. C. Hidalgo, *Phys. Rev. Lett.* **114**, 238002 (2015).



## SUPPLEMENTAL MATERIAL

### Effect of the overweight

In the main text, we have shown simulation results for a single value of the external force applied to the granular column. Our experimental data (see Fig. 1 in the main text), indicate that different weights applied to the piston lead to different speedup of the flow rate. We have carried out additional simulations with different overweights. The results are shown in Fig. 4. The particle flow rate [Fig. 4(a)], as it was seen in the experiments, increases more rapidly and at an earlier stage when heavier overweights are used. However,  $W_D/(PQ)$  as a function of  $N$  coincides for all values of the overweight [see Fig. 4(b)] and is reasonably well fitted by Eq. (5) in the main article. This confirms that the universal straight line holds for a wide range of external forces and the ordinate  $\alpha \approx 3.76$  is consistent with the value obtained for different granular materials (see Fig. 3 in the main article).

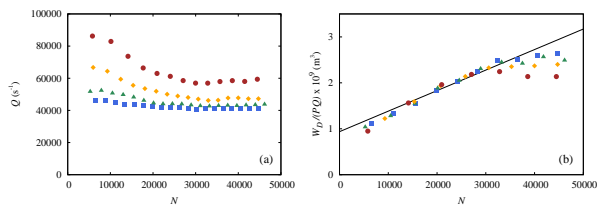


FIG. 4. (a)  $Q$  as a function of  $N$  for different pistons: 78 g (blue squares), 130 g (green triangles) and 262 g (orange diamonds) and 524 g (red circles). (b) Scaled dissipated power  $W_D/(PQ)$  as a function of  $N$ . The solid line corresponds to a fit using Eq. (5) in the main text with  $\alpha = 3.77$ .

### Effect of the silo radius

As we mentioned in the main text, Eq. (5) predicts that the slope of the universal straight line found for  $W_D/(PQ)$  as a function of  $N$  must depend on the silo

radius. To test this, we have carried out simulations of unforced discharges with silos of different radii  $R_s$ . Figure 5 displays the particle flow rate and scaled dissipated power. As we can see, the flow rate does not depend on the silo radius. Note that in Fig 5(a), the final stages of the discharge where the flow rate drops to zero is observed earlier for the wider silos since the plot is against  $N$  and not against the column height.

In Fig. 5(b), we show  $W_D/(PQ)$  as a function of  $N$ . As predicted by Eq. (5), the scaled dissipated power presents a different slope for each value of  $R_s$ . The solid lines in the figure correspond to the fit of Eq. (5). We recall here that the slope of the straight line is not fitted since Eq. (5) predicts its value. The fitted ordinate  $\alpha$  is rather insensitive to  $R_s$  in a first approximation. An increase of 66 % in  $R_s$  induces a 16 % reduction in  $\alpha$ . However, the values do vary and are somewhat higher than for the forced discharges (compare with Fig. 4(b)).

We speculate that the value of  $\alpha$  may depend on geometrical details such as the actual shape of the silo cross-section or the presence of a hopper-shaped base. There is also an additional effect (neglected in our analysis) due to the dissipation of the grains in contact with the piston. This makes the forced discharges slightly “more dissipative” than the unforced flows. These “second order” effects merit further study and may become crucial in specific applications.

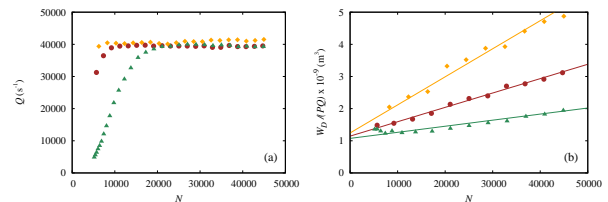


FIG. 5. (a)  $Q$  as a function of  $N$  during unforced discharges for different silo radius  $R_s$ : 0.012 mm (orange diamonds), 0.015 mm (red circles) and 0.020 mm (green triangles). (b) Scaled dissipated power  $W_D/(PQ)$  as a function of  $N$ . The solid lines correspond to a fit using Eq. (5) in the main text with  $\alpha = 5.0$  (orange), 4.59 (red) and 4.31 (green).